

# Thermo-mechanical Analysis of Conformally Coated QFNs for High Reliability Applications

Chunyan Yin, Stoyan Stoyanov, Chris Bailey and Paul Stewart

**Abstract**—The use of Quad Flat No-leads (QFNs) in high reliability applications is receiving increased interest. To address concerns of harsh working environments, conformal coatings are used to protect the components and associated printed circuit board (PCB). However, using conformal coatings can pose a reliability risk for the components on the PCB. This paper details an investigation into the effect of conformal coatings on the reliability of QFN second-level solder interconnections. Five QFN package types and two types of conformal coatings were investigated. In the experiments, a large population of QFN assemblies coated with conformal coatings were subjected to a thermal cycling test condition. These components, designed with daisy chain connections, were monitored during the thermal cycling tests and the exact time for failure to occur for each component was recorded and analyzed. Detailed finite element models for the tested QFN assemblies were developed, the inelastic strain energy density was used as the damage indicator to evaluate the impact of conformal coating on the solder joint reliability. Modelling results reveals that conformal coating plays a complex role in QFN solder joint reliability, the presence of conformal coating results in a reduction in the shear stress in the solder joint and plays a positive role in solder reliability, but it also induces more stress in the solder joint in the out-of-plane direction and plays a negative role. These two mechanisms are competing and the relative magnitude of them will determine the overall effect of conformal coating on solder joint reliability.

**Index Terms**— QFN, conformal coating, reliability, finite element analysis, thermal cycling

## I. INTRODUCTION

QFNs (Quad-Flat No Leads) are one of the most successful packages today in the consumer electronics market. Compared to other no-lead packages, they offer small form factor, good electrical and thermal performance, and are generally lower in cost [1-3]. Manufacturers of high reliability electronic systems, who rely on the commercial electronics supply chain for advanced packages, are showing increased interests in using QFNs in their systems in order to meet miniaturization and functionality goals [4].

This paragraph of the first footnote will contain the date on which you submitted your paper for review. It will also contain support information, including sponsor and financial support acknowledgment. For example, "This work was supported in part by the U.S. Department of Commerce under Grant BS123456."

The next few paragraphs should contain the authors' current affiliations, including current address and e-mail. For example, F. A. Author is with the

In applications such as avionic and aerospace electronics where high reliability is essential, conformal coatings are being used to provide extra protection to the printed circuit board (PCB) from harsh environments that may include dust, chemicals, vibration etc. [5-6]. Another benefit from the use of conformal coating is it can reduce the risk of tin-whiskers on pure tin surface finishes [7-10]. Although the thermal cycling reliability of QFNs has been previously studied [1-3], there is a lack of understanding about the impact of using conformal coating on the reliability of these components [4].

Conformal coating is a thin polymeric film which 'conforms' to the contours of a printed circuit board to protect the board and components. This coating can be applied onto the PCB using methods such as brushing, spraying and dipping, with a typical thickness of 30-130 $\mu$ m. When QFNs are conformably coated, the coating can penetrate under the package and fill the gap between the package and the PCB board. During thermal cycling, the coating expands or shrinks as temperature changes and has an impact on the mechanical behavior of the solder joints and hence their reliability. Previous experimental study [11] has identified that using a conformal coating can have significant impact on the solder reliability of QFNs. The cycles to failure of the solder joint could reduce from ~2,500 cycles for un-coated QFNs to 300 cycles for coated QFNs. However, in the work reported by Y. C Deng et.al. [12], it was found that using conformal coating actually improved the thermal mechanical reliability of QFN assemblies up to 1000 cycles. This indicates that conformal coating plays a complex role in the solder reliability of QFNs and the level of this impact could be dependent on the package size, coating properties etc. Although the impact of conformal coating on the reliability of QFNs were investigated using computational models by Vianco, et al. [4], the models used were simplified and there was lack of discussion about the solder behavior in such conformally coated QFNs.

In this paper, a comprehensive study was carried out to investigate the impact of using conformal coating on the

National Institute of Standards and Technology, Boulder, CO 80305 USA (e-mail: author@boulder.nist.gov).

S. B. Author, Jr., was with Rice University, Houston, TX 77005 USA. He is now with the Department of Physics, Colorado State University, Fort Collins, CO 80523 USA (e-mail: author@lamar.colostate.edu).

T. C. Author is with the Electrical Engineering Department, University of Colorado, Boulder, CO 80309 USA, on leave from the National Research Institute for Metals, Tsukuba, Japan (e-mail: author@nrim.go.jp).

Table 1. Geometry information of the tested QFN components

Ref no.	Type of QFN	Package image	Pin count	Pitch (mm)	Package dimension (mm)			Die size (mm)			Thickness of paddle (mm)	Paddle to package area ratio
					Length	Width	Thickness	Length	Width	Thickness		
P1	Plastic		32	0.5	5	5	0.75	3.2	3.2	0.15	0.2	0.48
P2	Plastic		38	0.5	5	7	0.75	2.9	4.9	0.2	0.2	0.46
P3	Plastic		64	0.5	9	9	0.75	5	5	0.2	0.2	0.63
P4	Plastic		80	0.5	12	12	0.85	8	8	0.25	0.2	0.55
C1	Ceramic		16	0.5	3	3	0.92	0.7	0.7	0.15		

reliability of QFNs. Both experimental and computational modeling methods were used; five types of QFNs (including plastic and ceramic QFNs) and two types of conformal coatings were investigated. Reliability testing was carried out for the selected components with or without a conformal coating and the results were statistically analyzed. Failure analysis was carried out to reveal the failure mode of the components and the findings were also used to validate the modeling results. For each component type, a detailed finite element model was developed and the solder damage accumulated over one thermal cycle was calculated and used as the damage indicator. The modeling results show that conformal coating plays a complex role in QFN solder joint reliability, a detailed discussion on this role is provided in the paper.

## II. RELIABILITY TESTING

### A. Components and Conformal Coatings

Five types of QFNs and two types of conformal coatings were selected and investigated in this work. The reference number and package geometric details for each QFN are provided in Table 1. The selected plastic QFNs varies in size, although they have similar internal construction, there is some variability in geometry factors such as the die to package ratio and the paddle to package ratio. The two types of conformal coatings (Coating A and Coating B) are made of different materials. Coating A is a polyurethane and Coating B is an acrylic. Figure 1 shows how the QFN component (P1) typically looks when it is coated with these conformal coatings.

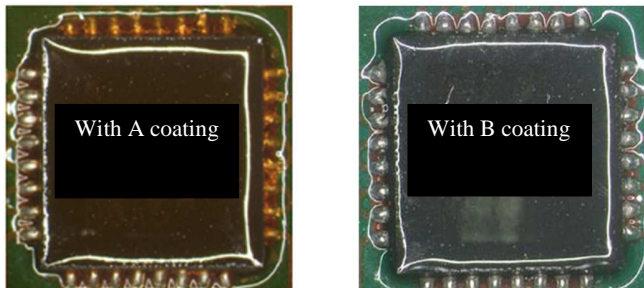


Fig. 1. P1QFN (5X5) component with one of the conformal coatings

### B. Experimental Procedure

A large population of QFN components, designed with daisy chain connections, were assembled onto FR4 PCB boards (2.61mm in thickness) with Sn62/Pb36/Ag2 solder. After that, one of the two conformal coatings was applied onto the PCB board using a manual spraying method and cured at a suggested curing temperature for a certain period of time. These assemblies were then subjected to thermal cycling test conditions of -25 to 100°C, with 10 minutes ramp and 10 minutes dwell. During the thermal cycling test, the daisy chains were continuously monitored by detectors and solder joint failures were recorded automatically with the cycle number and temperature at time of the failure. Test results were statistically analyzed and the cycles to failure for each type of package were obtained. After the thermal cycling tests, some of the samples were cross sectioned for failure mode analysis, and some of them went through a mechanical test in which the QFN component was removed from the PCB board to reveal the coating penetration levels underneath the package.

The test chamber used for this work and the PCBs with different types of QFNs are shown in Figure 2.

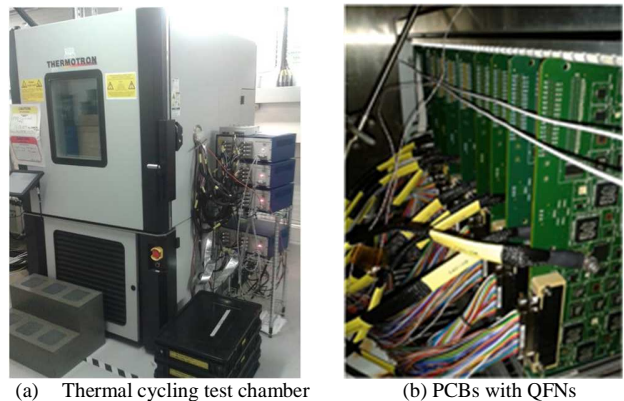


Fig. 2. Thermal cycling chamber and PCB boards with QFNs inside the chamber

### C. Experimental Results

Reliability test data of the QFN packages were analyzed using regression analysis to determine the Weibull shape factor ( $\beta$ ) and characteristic life ( $\eta$ ). The sample size was 30 for each case. The results are shown in Table 2, where the characteristic life reported corresponds to the number of cycles at which 63.2% of the population have failed. Two sets of life time data (with coating A or coating B) were obtained for QFN components P2, P3, P4 and C1. For component P1, extra data points were collected to look into the impact of stencil thickness (hence solder volume) on the reliability of QFNs. When a thinner (0.004" in thickness) stencil is used, the solder joint generally has a smaller solder stand-off height compared to the one printed using a thicker (0.005" in thickness) stencil.

Table 2. Experimentally measured life time for tested QFN packages

Case no.	Component no.	Coating type	Thickness of stencil	$\beta$	$\eta$
1	P1	A	0.005"	2.42	1593
2	P2	A	0.005"	3.25	1060
3	P3	A	0.005"	1.96	1886
4	P4	A	0.005"	2.51	1364
5	C1	A	0.005"	4.40	1048
6	P1	B	0.005"	7.49	2874
7	P2	B	0.005"	7.08	2264
8	P3	B	0.005"	4.34	2968
9	P4	B	0.005"	2.32	1661
10	C1	B	0.005"	3.86	1959
11	P1	No coating	0.004"	6.99	2118
12	P1	B	0.004"	7.37	2869

The results of component P1 show that both types of conformal coatings have significant impact on the reliability of QFNs. Compared to the no coating cases, when coating B is used, the lifetime of QFN assemblies is improved, while coating A has an opposite effect. The parameters such as the thickness of stencil show minor impact on component P1 (5x5) reliability when conformal coating is used. When compared to the other three plastic QFN types, the life time of the QFN generally decreases with the package size except for component P3 (9x9), which has the smallest die to package area ratio and biggest paddle to package area ratio among all QFN types. The ceramic QFN assembly shows shorter life time than most other plastic QFNs due to the larger CTE mismatch between the component and the PCB board.

The failure mode of such QFN assemblies was assessed using SEM and optical microscopy. It was confirmed that the failure was due to cracking in the peripheral solder joints, particularly at the corner of the package. The crack was found at the interface between the component pad and the solder joint and propagated into the solder fillet, as shown in Figure 3.

The coating penetration level underneath the package was assessed for all package types through a mechanical test. The component was removed from the PCB board to reveal the coating penetration levels. Results showed that coating penetration level varies with the type of conformal coating and the package type/size. For the two conformal coating types used

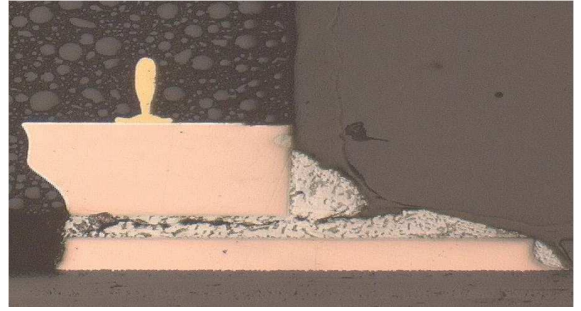


Fig. 3. Microscope image showing a crack in a QFN solder joint

in this study, coating A tends to penetrate further underneath the package. As an example, Figure 4 shows the coating A penetrated underneath the package P1 and the coating profile on the side and top surface of the package.

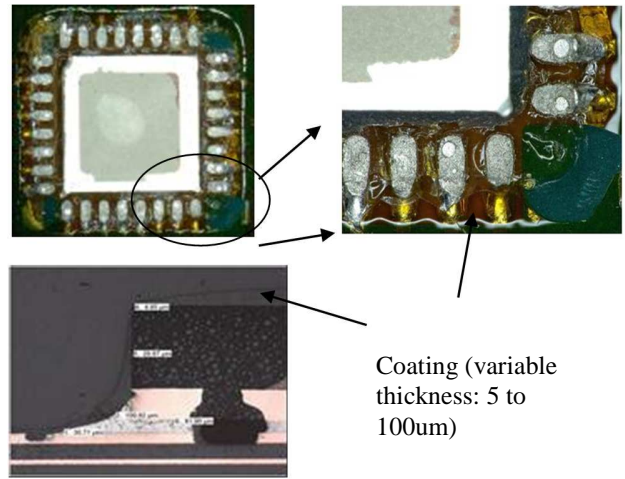


Fig. 4. Coating A penetration level and coating profile (Component P1)

### III. FINITE ELEMENT ANALYSIS

Package characterization was firstly carried out to gather the data on package construction, geometry and materials. SEM-EDX, cross-sectional metallurgy and 3D CT scan were used to reveal the internal construction of each package. Together with the information collected from the supplier, technical datasheets, experimentally measured solder stand-off height and coating profiles, a detailed 3-dimensional model was developed for each QFN type. Using the models developed, thermal mechanical analysis was carried out to predict the damage distribution in the solder joint during the thermal cycling test. The overall modelling workflow is detailed in Figure 5. ANSYS software was used for all aspects of the modelling process: pre-processing, solution, and post-processing.

#### A. Model Development

Due to the symmetry of the package, a quarter model of the QFN assembly was developed to save computation time. For example, the mesh model developed for component P1 without the conformal coating is shown in Figure 6. The terminations of

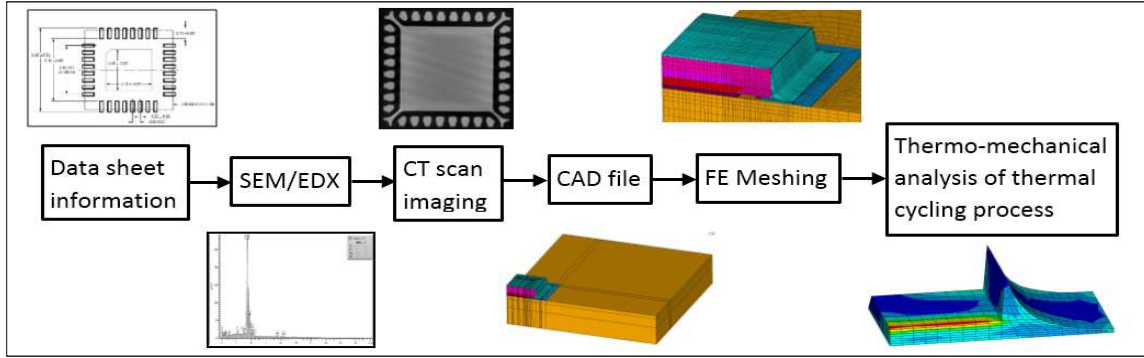


Fig. 5. Modelling workflow

the QFN component are made of copper and the component is connected to the PCB through a center solder joint and peripheral solder joints. The impact of solder mask on solder reliability is normally ignored in modelling non-coated QFNs; however, in this case as this material is sitting in the coating penetration area, they have been included into the model. The

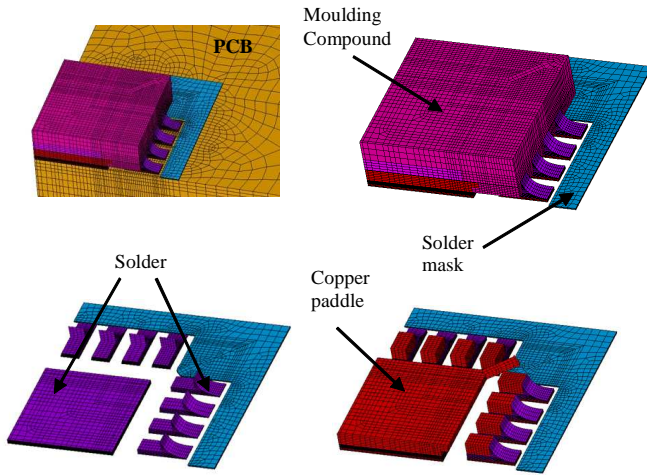


Fig. 6. Mesh model of non-coated QFN P1 assembly

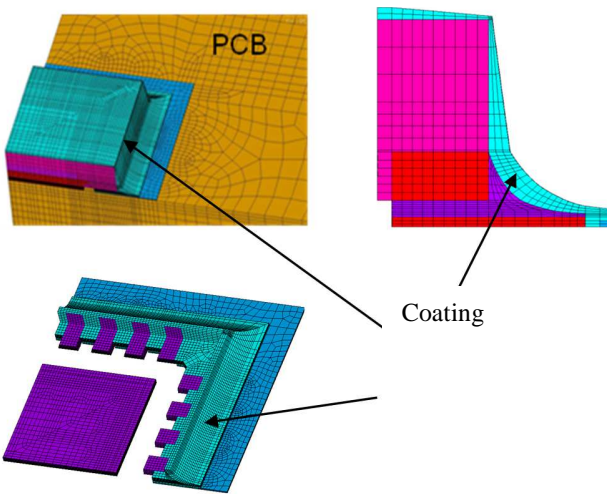


Fig. 7. Mesh model of conformably coated QFN P1 assembly

shapes of each solder joint were defined using the measured solder stand-off height and manufacturer's target solder volume to capture a realistic shape.

In comparison to Figure 6, Figure 7 shows the quarter model developed for the same component (P1) when conformal coating is used. The component is covered by the conformal coating and there is coating penetration underneath the package. The coating profile on the top and side of the components was taken from experimental measurements, it has a variable thickness ranging from 5 to 100um. The coating penetration underneath each package was defined using measurement data and with assumptions that the perimeter of the coating seepage underneath the package is in a regular shape (straight line) and symmetrical, and the coating connects the bottom surface of the component to the top surface of the PCB. There was a trend with coating B for more coating to accumulate in the corner area of the package, than at other terminations, and this has been included into the model as well.

#### B. Constitutive Equation for Modeling Solders

The mechanical properties of a solder material are highly influenced by its creep behaviour when its homologous temperature is getting close or above 0.5 [13, 14]. The homologous temperature is defined as the ratio of the operating and melting temperatures of the solders in absolute scale. As SnPbAg solder (Sn: 62%, Pb: 36%, Ag: 2%) has a low melting point of about 180°C, it has a homologous temperature greater than 0.54 at -25°C and 0.82 at 100°C, the creep behaviour of this solder material needs to be modelled and this can be achieved by using a suitable constitutive model for solders. In this paper the Anand constitutive model, which is available in ANSYS code, was used to represent the inelastic deformation behavior of the solder. In the Anand model, plasticity and creep are unified and described by the same set of flow and evolution relations [14].

Anand's model can be broken into a flow equation and three evolution equations, as shown below

Flow equation:

$$\frac{d\epsilon_p}{dt} = A \left[ \sinh \left( \xi \frac{\sigma}{s} \right) \right]^{\frac{1}{m}} \exp \left( -\frac{Q}{RT} \right) \quad (1)$$

Evolution equations:

$$\frac{ds}{dt} = \{h_0(B)\}^a \left\{ \frac{B}{|B|} \right\} \frac{d\epsilon_p}{dt} \quad (2)$$

$$B = 1 - \frac{s}{s^*} \quad (3)$$

$$s^* = \hat{s} \left\{ \frac{d\epsilon_p}{dt} \exp\left(-\frac{Q}{RT}\right) \right\}^n \quad (4)$$

There are 9 constants to define before the Anand model can be used, as shown in Table 3. The value of these input parameters can be obtained through a set of experimental tests, or a correlation process to match the results of the Anand model with other types of constitutive models. In this work, the value of these input parameters for SnPbAg solder material were taken from previous published work and they were generated through a correlation process using the Darveaux's constitutive models [15].

Table 3. Anand Constants for ANSYS 62Sn36Pb2Ag Solder [15]

Input parameter	Value	Definition
$s_0$ (MPa)	12.41	Initial value of deformation resistance
Q/R (1/K)	9400	Activation energy/boltzmann's constant
A(1/s)	4E06	Pre-exponential factor
$\xi$	1.5	Multiplier of stress
m	0.303	Strain rate sensitivity of stress
$h_0$ (MPa)	1379	Hardening constant
$\hat{s}$ (MPa)	13.79	Coefficient for deformation resistance saturation value
n	0.07	Strain rate sensitivity of saturation (deformation resistance) value
a	1.3	Strain rate sensitivity of hardening

### C. Material Data and Loading Conditions

Thermo-mechanical analysis (TMA) and Dynamic-mechanical Analysis (DMA) were carried out to measure the temperature dependent material properties (modulus, CTE) for the conformal coatings above and below their glass transition temperature, the data are listed in Table 4.

Table 4. Experimentally measured material data for conformal coating

Conformal coating	Young's Modulus (MPa)	CTE(ppm/°C)	Tg(°C)
A coating	3840 at -55°C	193 (< T <sub>g</sub> ) 340 (> T <sub>g</sub> )	26
	3310 at -20°C		
	3020 at -0°C		
	2590 at 20°C		
	1950 at 40°C		
	820 at 60°C		
	30 at 80°C		
	6 at 100°C		
B coating	7950 at -55°C	112.9 (< T <sub>g</sub> ) 300 (> T <sub>g</sub> )	43.2
	6490 at -20°C		
	5370 at -0°C		
	3690 at 20°C		
	1180 at 40°C		
	50 at 60°C		
	7 at 80°C		
	3 at 93°C		

Table 5. Material data for plastic QFNs

Material	Modulus (MPa)	CTE (ppm/°C)	Poisson's ratio	T <sub>g</sub> (°C)
Solder	40000 at -50°C	26	0.4	
	21800 at 60°C			
	12800 at 100°C			
Copper	120000	16.6	0.34	
Solder mask	3800	70	0.4	
Moulding (for Comp. P1, P2 and P3)	29006 at 25°C	7 (<T <sub>g</sub> ) 34 (>T <sub>g</sub> )	0.4	135
	920 at 260°C			
Moulding (for Comp. P4)	27000	8 (<T <sub>g</sub> ) 34 (>T <sub>g</sub> )	0.4	125
Die attach	9356 at -65°C	61 (<T <sub>g</sub> ) 195 (>T <sub>g</sub> )	0.4	241
	7840 at 25°C			
	6337 at 100°C			
	5092 at 150°C			
	3356 at 200°C			
PCB	22000	16 (x-y) 39 (z)	0.35	159
Silicon	163000	2.69	0.28	

Table 6. Material data for ceramic QFN

Material	Modulus (MPa)	CTE (ppm/°C)	Poisson's ratio	T <sub>g</sub> (°C)
Solder	40000 at -50°C	26	0.4	
	21800 at 60°C			
	12800 at 100°C			
Copper	120000	16.6	0.34	
Solder mask	3800	70	0.4	
Body	280000	6.8	0.3	
Die attach	8400 at -65°C	50 (<T <sub>g</sub> ) 200 (>T <sub>g</sub> )	0.4	103
	7300 at 25°C			
	5400 at -10°C			
	540 at 150°C			
	390 at 200°C			
PCB	22000	16 (x-y) 39 (z)	0.35	159
GaAs Die	110000	6.0	0.3	
Tungsten	400000	4.5	0.3	
Lid Attach	1400	110(<T <sub>g</sub> ) 145(>T <sub>g</sub> )	0.4	150
Lid	280000	6.8	0.3	

Data for all other materials in the assembly was obtained from the component supplier, technical datasheets or public domain. All materials are assumed as linear elastic except solder where nonlinear material properties are used. Tables 5 and 6 summarizes the material data used for the materials in the plastic and ceramic QFNs respectively.

The thermal load in the simulations was defined to match the thermal cycling conditions used in the experimental tests and is

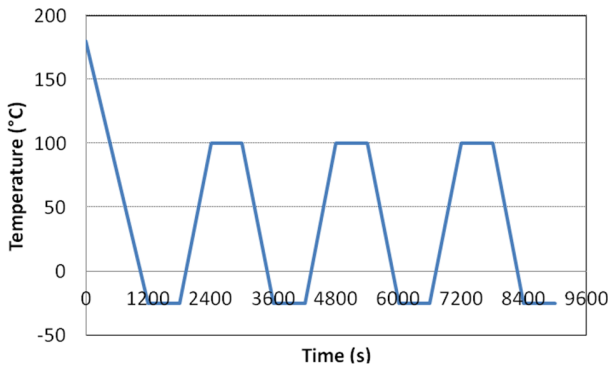


Fig. 8. Thermal load used in simulations

shown in Figure 8. Temperature starts at 180°C which is the solder joint solidification temperature, to include the residual stress due to reflow. The curing (stress free) temperatures of coatings A and B are provided by the manufacturer and they are 90°C and 22°C respectively. The stress free temperature of the PCB is 170°C and 145°C for the materials inside the component. The stress free temperature for the solder material is 180°C.

#### D. Damage Distribution and Results

The inelastic strain energy density was used as an indicator of the damage induced in the second-level solder interconnects under the applied thermal cycling load. Figure 9 shows the damage distribution in the solder joints of component P1 (P5X5) with and without conformal coating applied. The results were taken at the end of the third temperature cycle (at -25°C) in both cases, and it is shown that the critical solder joint is located at the package corner which has the largest distance to the neutral point (DNP). The crack is likely to occur along the

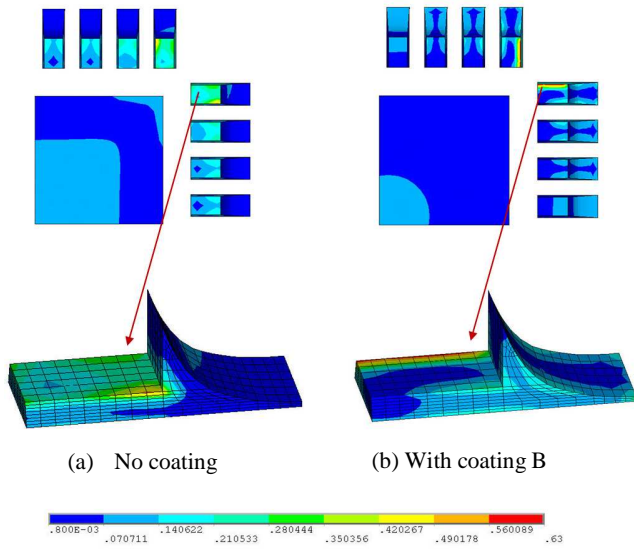


Fig. 9. Simulation predicted solder damage in P1 assembly (unit: MPa)

interface between component pad and the solder, and propagate into the solder fillet. The existence of conformal coating has changed the damage distribution within the corner solder joint, higher damage is seen at the interface between the solder joint, component pad and the conformal coating.

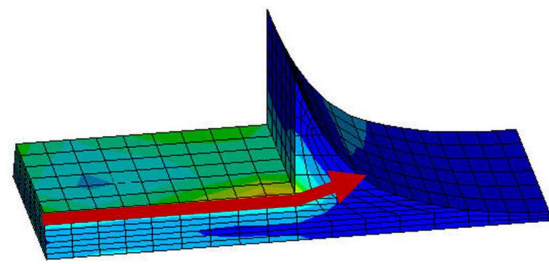


Fig. 10. Elements used for calculating the volume averaged damage

The volume averaged damage  $\Delta W_{ave}$  accumulated within the third temperature cycle in the solder joint was calculated for the corner solder joint using the top three layers of elements (~25µm in thickness) under the component pad and some elements in the solder fillet, as shown in the Figure 10. This was used as the damage indicator to assess the solder reliability. For component P1 shown in Figure 9, although using conformal coating has induced higher damage at the interface between the coating and the joint, the volume averaged damage for the selected elements is lower when conformal coating B is used.

Simulations were carried out for all the five types of QFN packages with or without conformal coating. The predicted solder damage is summarized in Figure 11. The results show that conformal coatings have a significant impact on the solder reliability of QFNs. The magnitude of this impact is dependent on the package size and coating properties. However, using conformal coating does not always increase QFN solder damage. Compared to non-coated cases, when coating B is used, the damage in the solder joint is reduced in the smaller packages (P1, P2, P3, C1), but increased in the larger package (P4). When coating A is used, the damage in the solder joint increased for all the packages. Simulation results were also

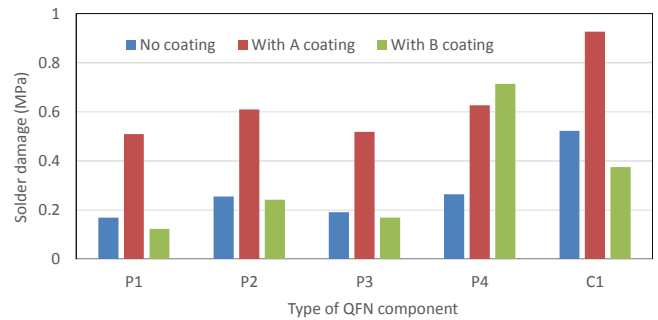


Fig. 11. Volume averaged damage for all tested QFNs

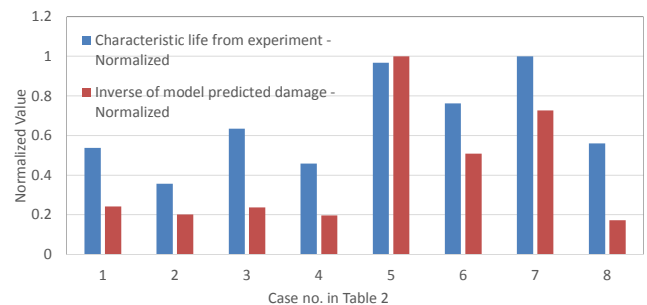


Fig. 12. Trend analysis of the inverse of model predicted damage and experimentally measured life time (normalized data were used)

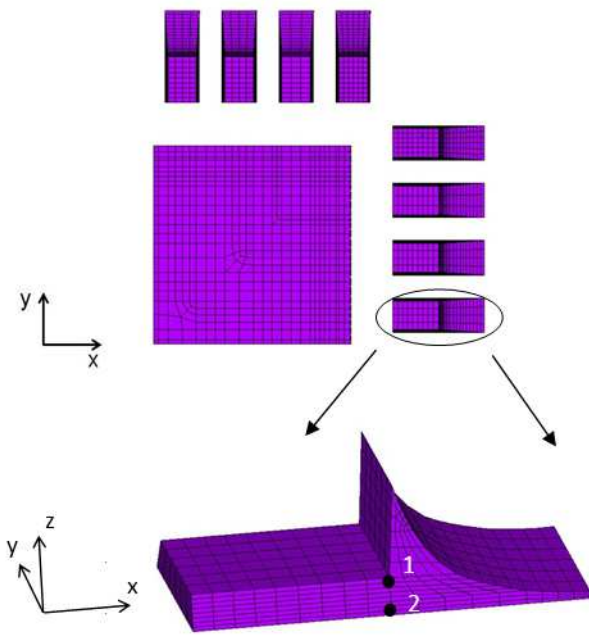


Fig.13. Displacement measurement at extreme temperature compared to the experimental results for the cases where the test data are available. As shown in Figure 12, a trend analysis was carried out using the normalized experimental data and the inverse of modeling predicted damage for the four types of plastic QFNs corresponding to the cases from no 1 to 8 in Table 2. The results show that the inverse of the simulations predict damage generally follows the same trend as the experimentally measured cycle to failure.

### E. Solder Joint Displacement Analysis

In order to have a better understanding of QFN solder behavior, the displacement within a solder joint of component P1 was analyzed and the results were compared between the coating B and non-coated cases at  $-25^{\circ}\text{C}$  (extreme temperature) in the third thermal cycle of experimental test. This analysis was carried out using the center solder joint for the P1 package.

As shown in Figure 14, two locations (node 1 and node 2) were picked up for this analysis. Node 1 is located at the interface between the component and solder joint, and node 2 has the same coordinate as node 1 in X direction but located at the interface between solder joint and PCB pad. The difference

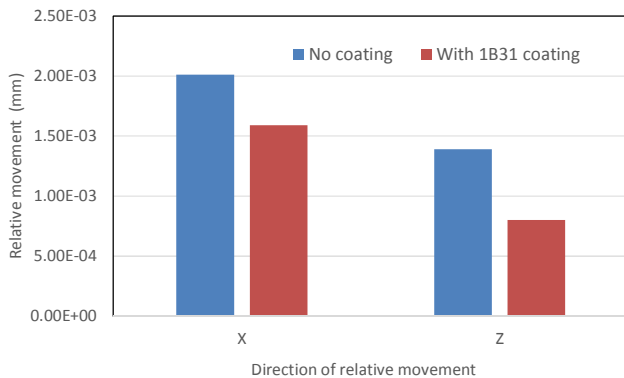


Fig. 14. Difference between the displacements at node 1 and node 2

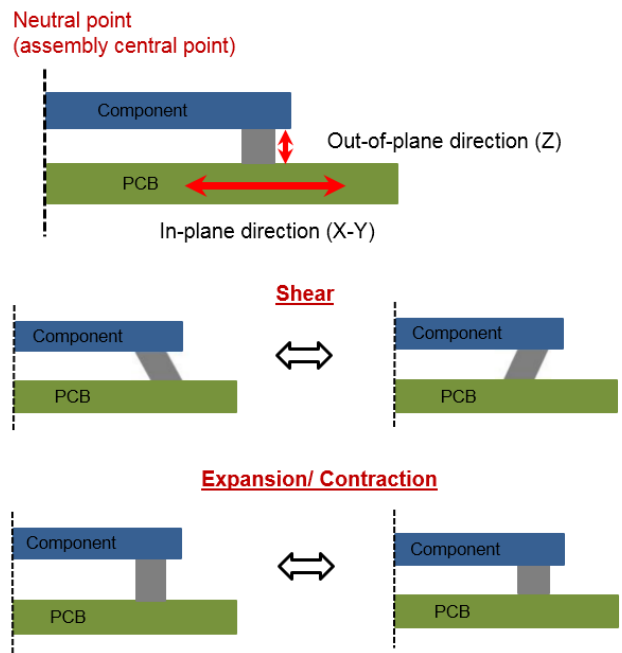


Fig. 15. Solder movement in non-coated QFNs

in displacements between node 1 and node 2 represents the relative movement in the solder joint. When temperature changes, the solder joint deforms and the relative movement between the two nodes in x-direction reflects the magnitude of shear strain in the solder joint. The relative movement between the two nodes in z-direction reflects the level of solder movement in the out-of-plane direction when temperature changes.

As shown in Figure 14, the presence of conformal coating B reduces the relative movement between the two selected node locations in the solder joint in both in-plane (X-Y) and out-of-plane (Z) directions. This indicates that the presence of coating B reduces the shear movement in the solder joint and also constrains the solder joint from its free movement in the out-of-plane direction when temperature changes.

### F. Discussions on Solder Behavior

During thermal cycling test, movement in the solder joint can be explained in two directions: in-plane and out-of-plane, as illustrated in Figure 15. In the in-plane direction, due to the CTE mismatch between the PCB and component, the materials expand/contract at different scale when temperature changes, this induces shear strain/stress in the solder joint and the joints furthest from the natural point are exposed to the highest shear stress. In the out-of-plane direction, solder joints can expand/contract freely. Hence, the major failure mechanism of the non-coated QFNs during the thermal cycling test is the shear stress induced by the CTE mismatch between the PCB and component.

When conformal coating is used, the presence of conformal coating reduces the relative movement between the component and PCB in the in-plane direction, helping to reduce the shear strain/stress in the solder joint, and hence improves the solder reliability (this is a positive role). In the out-of-plane direction,

the presence of the conformal coating constrains solder joint free movement when temperature changes, inducing stresses in the solder joint and consequently reduces the solder reliability (this is a negative role). These two mechanisms compete and the relative magnitude of these mechanisms will determine the overall effect of conformal coating. Apparently, the level of the impact depends on the package size, coating penetration level and coating properties.

#### IV. CONCLUSIONS

A comprehensive multidisciplinary study was undertaken to investigate the impact of using conformal coatings on the solder joint reliability of QFNs. Five types of QFN components with different size and construction were investigated, together with two types of conformal coatings. Key findings are:

- 1) The level of penetration of conformal coating has to be accessed in order to generate accurate finite element models. Our approach is to use CT scans to obtain package construction and optical measurements for coating penetration. These data was inserted into the finite element models.
- 2) Conformal coatings have a significant impact on QFN reliability. The magnitude of this impact varies with coating properties and package size.
- 3) Generally conformal coating is expected to reduce lifetime of QFN solder joints. This investigation has confirmed this, but in some cases the use of coating can have a positive impact on solder joint life. This is particularly for low CTE coatings used with small packages.
- 4) Conformal coatings influence the behavior of the QFN package in the following ways: (a) reduce shear stress/strain in solder due to CTE Miss-match: this is a positive role; (b) constrains the out-of-plane deformation of the solder joint: this is a negative role.
- 5) The impact of conformal coatings on QFN solder joint reliability is governed by the relative magnitude of these two mechanisms.

Finite element modelling has helped gain significant insights into the influence that conformal coatings can have on QFN solder joint behaviour. Model predictions agree with the trends found in the test data.

#### ACKNOWLEDGMENT

This research has been funded by the Defense Microelectronics Activity (DMEA), USA, under "Reliability Prediction Analysis for Solder Joint Integrity" program, with Contract number: H94003-04-D-0070. The authors would like to acknowledge the experimental work carried out by Leonardo MW Ltd- Airborne & Space Systems Division (Edinburgh, Scotland), and also thank John Roulston from Scimus Solutions Ltd for the input and the overall support.

#### REFERENCES

[1] Li Li, "Reliability Modelling and Testing of Advanced QFN Packages", proceedings of 2013 ECTC conference, pp. 725-730.

[2] Ahmer Syed and WonJoon Kang, "Board Level Assembly and Reliability Considerations for QFN Type Packages", proceedings of 2003 SMTA conference, USA.

[3] Guofeng Xia, Fei Qin, Wenhui Zhu et al. "Comparative Analysis of Reliability Between Dual-row and Conventional QFN Packages", proceedings of 2012 Int. Conf. on Electronic Packaging Technology & High Density Packaging, pp. 616-619.

[4] Paul Vianco, Michael K Neilsen, "Thermal Mechanical Fatigue of a 56 I/O Plastic Quad-Flat NoLead (PQFN) Packaging", proceedings of SMTA International Conference, Rosemont, 2015, pp. 85-94.

[5] Maxim Serebreni, Ross Wilcoxon, Dave Hillman, Nathan Blattau and Craig Hillman, "The Effect of Improper Conformal Coating on SnPb and Pb-free BGA Solder Joints during Thermal Cycling: Experiments and Modeling", proceedings of the 33rd SEMI-THERM Symposium, 2017, pp. 40-47.

[6] Kati Kokko, Laura Frisk and Pekka Heino, "Thermal Cycling of Flip Chip on FR-4 and PI substrate with Parylene C coating", Soldering & Surface Mount Technology, volume 22, 2010, pp. 42-48.

[7] Stoyan Stoyanov, Chris Bailey etc., "Modelling Methodology for Thermal Analysis of Hot Solder Dip Process", Journal of Microelectronics Reliability, Vol. 53, 2013, pp. 1055-1067.

[8] Thomas A. Woodrow, Eugene A. Legbury "Evaluation of Conformal Coatings as a Tin-Whisker Mitigation Strategy Part II", proceedings of 2006 SMTA International Conference, Rosemont, IL, pp 1-33.

[9] Michael Osterman, "Assessment of Tin Whisker Mitigation for Conformally Coated SnPb Assemblies" [online]. <https://web.calce.umd.edu/tin-whiskers/presentations/CALCE-conformal-coating-study.pdf>

[10] Guangbin Dou, D.P. Webb, et al., "Current Leakage Failure of Conformally Coated Electronic Assemblies", Proceedings of 2008 IEEE conference on Electronics System-Integration Technology Conference, London, pp. 1213-1218.

[11] Greg Caswell, Cheryl Tulkoff and Dr. Nathan Blattau, "The Effect of Coating and Potting on the Reliability of QFN Devices," [Online]. <http://www.m-coat.com/ICSR%20Slides-Caswell%20%5BCompatibility%20Mode%5D.pdf>

[12] Deng Yun Chen, Michael Osterman, "Reliability of Conformal Coated Surface Mount Packages", Proceedings of 2016 IEEE Accelerated Stress Testing and Reliability Conference (ASTR), Pensacola Beach, FL, USA, pp. 1-5.

[13] X.Q.Shi, Z.P.Wang, W. Zhou, J.H.L.Pang and Q.J. Yang, "A New Creep Constitutive Model for Eutectic Solder Alloy", Journal of Electronic Packaging, Transactions of the ASME, vol.124, June 2002, pp. 85-90.

[14] L. Anand, "Constitutive Equations for the Rate-Dependent Deformation of Metals at Elevated Temperature", Journal of Engineering Materials and Technology, Transactions of the ASME, 104(1), 1982, pp.12-17.

- [15] R. Darveaux, "Effect of Simulation Methodology on Solder Joint Crack Growth Correlation", Proceedings of ECTC 2000, pp.1048-1058.

**Chunyan Yin** received her BEng and MEng degrees in Material Engineering from Harbin Institute of Technology, Harbin, China, in 1999 and 2001, respectively, and the PhD degree in Computational Science and Engineering at University of Greenwich, London, United Kingdom, in 2006.

In 2001, she worked as a Research Assistant at City University of Hong Kong undertaking research into the failures of microelectronic components. Since 2007, she has worked as a Research Fellow and then a Lecturer at University of Greenwich, London, UK. During this time, she has worked on a number of government- and industry-funded projects developing models to predict the reliability of micro and power electronic components. Her research interests include physics-of-failure modelling, statistical analysis for reliability assessment, and prognostic and health management of electronics. She has published over 50 peer-reviewed papers in these areas.

**Stoyan Stoyanov** (M'08–SM'16) received the BSc degree in mathematics from Sofia University, Bulgaria in 1994 and the MSc degree in applied mathematics from the same institution in 1996. He has obtained his PhD degree in computational engineering at University of Greenwich, London, United Kingdom, in 2004. Since 2004, he is a member of the Computational Mechanics and Reliability Group (CMRG) at the School of Computing and Mathematical Sciences at University of Greenwich, London, UK.

In 2009 he was promoted from the position of Senior Research Fellow to Reader in Computational Engineering and Optimization. His research interests include the development and application of modelling and simulation tools for numerical analysis of the performance and reliability of electronics products and microsystems, physics-of-failure modelling, computational intelligence for data-driven and prognostics modelling, additive manufacturing and design optimization. He has published over 90 peer-reviewed papers.

Dr. Stoyanov is a member of the IEEE Electronics Packaging Society and a member of the Steering Committee of the IEEE International Spring Seminar on Electronics Technology.

**Chris Bailey** (M'03-SM'05) received his PhD in Computational Modelling from Thames Polytechnic, UK, in 1988, and an MBA in Technology Management from the Open University, UK, in 1996. He then joined Carnegie Mellon University as a Research Fellow within the Department of Materials Science from 1988-1991. Returning to the UK, he joined the University of Greenwich in London as Senior Research Fellow and in 2001 he obtained a Professorship in Computational Mechanics and Reliability.

Professor Bailey is Director of the Computational Mechanics and Reliability Group at the University of Greenwich, London, United Kingdom. His research interests include Prognostics and Health Management, Engineering Reliability, Embedded and Smart Systems, Optimization, Computational Mechanics,

Multi-physics modelling, Maritime Engineering, Structural Analysis, Micro and Nano Systems and Additive Manufacturing. He has published over 250 papers in the field of modelling and reliability of micro-technology based processes and products and consults with a number of companies worldwide.

Professor Bailey is president-elect on the board of governors of IEEE-EPS, member of the Heterogeneous Integration Roadmap team, Chair of the UK&RI IEEE EPS/Reliability chapter, and an associate editor of the IEEE CPMT Transactions. He is also a member of several IEEE conference committees including EuroSime, ESTC and EPTC. He is also an executive member of the EPSRC funded Centre for Power Electronics in UK.

**Paul Stewart** received a BSc degree (Honours) in electronic and electrical engineering from Robert Gordon University (RGU), Scotland in 1986 and an MBA from Edinburgh University Business School in 1999. He has worked for Leonardo MW Ltd, Edinburgh (and its previous incarnations) for 31 years in a number of engineering roles, primarily concerned with product reliability and product safety.

Since 2006, he has been Engineering Lead for lead-free design and in 2013 became the Interconnects group Engineering Lead. His research interests include lead-free manufacturing, reliability of electronics products and physics-of-failure.